Research Article | Vol. 29, No. 22 / 25 Oct 2021 / Optics Express 36379
Optics EXPRESS

Molecular dynamic investigation of ethanol-water mixture by terahertz-induced Kerr effect

HANG ZHAO,[1,2] YONG TAN,[1,3] RUI ZHANG,[4,7] YUEJIN ZHAO,[1,2,8] CUNLIN ZHANG,[5] XI-CHENG ZHANG,[6] AND LIANGLIANG ZHANG[5,9]

[1]*Beijing Key Laboratory for Precision Optoelectronic Measurement Instrument and Technology, School of Optics and Photonics, Beijing Institute of Technology, Beijing 100081, China*
[2]*Yangtze Delta Region Academy of Beijing Institute of Technology, Jiaxing 314019, China*
[3]*Research Center for Metamaterials, Wuzhen Laboratory, Jiaxing 314500, China*
[4]*Shenzhen Institutes of Advanced Technology, Chinese Academy of Sciences, Shenzhen 518055, China*
[5]*Key Laboratory of Terahertz Optoelectronics (MoE), Department of Physics, Capital Normal University, Beijing 100048, China*
[6]*The Institute of Optics, University of Rochester, Rochester, NY 14627, USA*
[7]*rui.zhang1@siat.ac.cn*
[8]*yjzhao@bit.edu.cn*
[9]*liangliang_zhang@cnu.edu.cn*

Abstract: The terahertz Kerr effect (TKE) spectroscopy provides time-resolved measurement of low-frequency molecular motions of liquids. Here, the intense broadband terahertz (THz) pulses resonantly excite multiple molecular modes in pure ethanol and ethanol-water mixtures. For pure ethanol, the obtained unipolar TKE response contains the molecular relaxation information extending over tens of picoseconds, which originates from the coupling between the permanent molecular dipole moment of ethanol and the THz electric field. For ethanol-water mixtures with different molar proportions, the results observed on the sub-picosecond time scale can always be divided into the linear superposition of the TKE signals of pure ethanol and water. Under the observation time window over tens of picoseconds (after 1 picosecond), the relative molecular contribution of ethanol in the mixture changes nonlinearly with the increase of water molecules, implying the complex structural perturbation of ethanol hydrogen bond network in the mixture. This work provides a new perspective for further investigation on the hydrogen bond network structure and dynamics in aqueous amphiphilic solutions.

1. Introduction

The low-frequency molecular motions of hydrogen bond liquids, such as intermolecular hydrogen bond vibration, single-molecule reorientation and coordinated rearrangement of hydrogen bond system, occur on the time scale from femtoseconds to picoseconds [1–5]. These molecular motions are closely related to the structural dynamics of liquids, which have important effects on the corresponding chemicophysical properties and biological activities [6,7]. Water and alcohols are classic hydrogen bond liquids and have attracted extensive attention from researchers in the past two decades. In particular, as the simplest chemically amphiphilic aqueous solutions, alcohol-water mixtures, are considered as the reference for exploring molecular interactions in biological processes [8]. A large number of techniques, such as Raman, infrared, dielectric, and optical Kerr effect spectroscopy, have been applied to determine the transformation of some macroscopic parameters related to the structure of alcohol-water mixtures [9–16]. For example, in the ethanol-water solution, the parameters of excess enthalpy, diffusivity, viscosity and heat capacity exhibit maximum or minimum values at a certain ethanol molar fraction, which is caused by the interaction of hydrogen bonds in the mixture [16–19]. However, because

#439954 https://doi.org/10.1364/OE.439954
Journal © 2021 Received 11 Aug 2021; revised 6 Oct 2021; accepted 7 Oct 2021; published 20 Oct 2021

Optics EXPRESS

of the complexity of intermolecular interactions and large spectral overlap of relevant motion modes (such as relaxation processes and intermolecular modes), the accurate assessment of low-frequency molecular dynamics and systematic observation of hydrogen bond network in alcohol-water mixtures are still challenging.

More recently, terahertz Kerr effect (TKE) spectroscopy technology provides a new perspective to investigate the low-frequency molecular motions in liquids [20–24]. As the terahertz (THz) field can resonantly drive the rotation of a single molecule or the collective low-frequency molecular motions, a strong response with relatively high signal-to-noise ratio for molecular dynamics in liquid can be achieved. Therefore, the use of this novel TKE technique to observe the low-frequency molecular motions in alcohol-water mixtures is highly desired and essential for understanding the hydrogen bond dynamics at the microscopic level [25–27]. In particular, in 2018 Kampfrath et al. used the intense THz pulses centered at ~1 THz to excite methanol and obtained the unipolar TKE signal. They concluded that the V_1 vibrational mode (~1.7 THz) associated with the fluctuation of the methyl group is mainly isotropic and there is a week intermolecular coupling between the re-orientational relaxation and vibrational mode by THz pulse excitation [22]. Most recently, our group used broadband THz pulses to induce the Kerr effect in liquid water [23] and ionic aqueous solutions [24], and successfully detected the bipolar anisotropic responses originated from the intermolecular hydrogen bond vibration modes under resonant excitation. These latest experiments provide strong evidence and new perspective for further investigation of hydrogen bond dynamics in alcohol-water solutions. Nonetheless, to the best of our knowledge, the study of THz-driven Kerr effect in alcohol-water mixture has not been reported so far.

Here, we use the intense broadband THz pulse (peak electric field strength of ~15.5 MV/cm, center frequency of 3.9 THz, frequency range of 1~10 THz) to excite the ethanol and the ethanol-water mixed solutions with different molar proportions, and observe the time-resolved evolution of the transient birefringence. We analyze the potential microscopic origins that contribute to the polarizability anisotropy. For ethanol-water mixtures with different molar proportions, we extract the concentration-related contribution coefficients of pure ethanol and water on the sub-picosecond timescale and the relative amplitudes of the molecular motions under the observation time window over tens of picoseconds (after 1 ps). In addition, we find that the relative molecular contribution of ethanol in the ethanol-water mixture exhibits a maximum value at a certain molar proportion, which is caused by the destruction of the structure related to the hydrogen bond chain of ethanol. The application of TKE technology in ethanol-water mixture can provide a basic reference for understanding the interactions of different hydrogen bond liquids and facilitate to consummate the theoretical model of hydrogen bond dynamics.

2. Experimental results and theoretical analysis

The schematic diagram of the experimental setup is shown in Fig. 1(a). We used an organic 4-N, N-dimethylamino-4'-N'-methyl stilbene toluene sulfonic acid (DAST) crystal as the THz source [28], which was pumped with the 1550 nm femtosecond laser pulses (repetition rate of 1 KHz) produced by an optical parametric amplifier (OPA, Spectra Physics). The generated linearly polarized THz pump pulse was reflected by an off-axis parabolic mirror with focal length of 50.8 mm and focused onto the liquid sample. A set of low-pass THz filters with cut-off frequency of 18 THz was used to filter out the residual NIR. The THz-induced transient birefringence was detected by the time-delayed 45° polarized optical probe pulse with wavelength of 800 nm. The induced refractive index change Δn through the liquid film can be expressed by the phase shift $\Delta\varphi$ [20] measured by the classic electro-optical sampling (EOS) method with a balanced photodiode detector (PDB210A/M, Thorlabs), namely:

$$\Delta\varphi(t) = \frac{2\pi}{\lambda}\int_0^l \Delta n(z,t)dz \tag{1}$$

Optics EXPRESS

where l represents the thickness of the liquid sample. Δn denotes the difference of the refractive index changes along two major axes. In particular, we used a stable free-flowing liquid film system to avoid the additional background response and heating effect in traditional window materials. This system for generation of ultra-thin liquid film was consisted of two parallel 100 μm-diameter aluminum wires separated by ~5 mm. Liquid water, ethanol and ethanol-water mixtures used in this work had a thickness of 90 ± 4 μm by controlling the flow regulating valve, which was measured and calibrated by an optical second harmonic intensity autocorrelator [29]. We obtained the ultra-pure water (σ <0.1 μS/cm) from a lab-based purification system and purchased the ethanol with >99.8% purity from HUSHI (CHN). During all measurements, the surrounding environment is held at a constant temperature of 22 ± 1 °C. We used electro-optical sampling with 100 μm GaP to obtain the THz electric field waveform, and reconstructed the measured waveform with a full complex response function [23]. In addition, the intense THz pulse would saturate the GaP response. Therefore, we used the TKE signal of diamond to calibrate the THz electric field strength [23,30,31]. As a result, we obtained an intense and broadband THz pump pulse with peak electric field strength of 15.5 MV/cm and bandwidth over the range of 1~10 THz with a center frequency of 3.9 THz, as shown by the red line in Fig. 1(b).

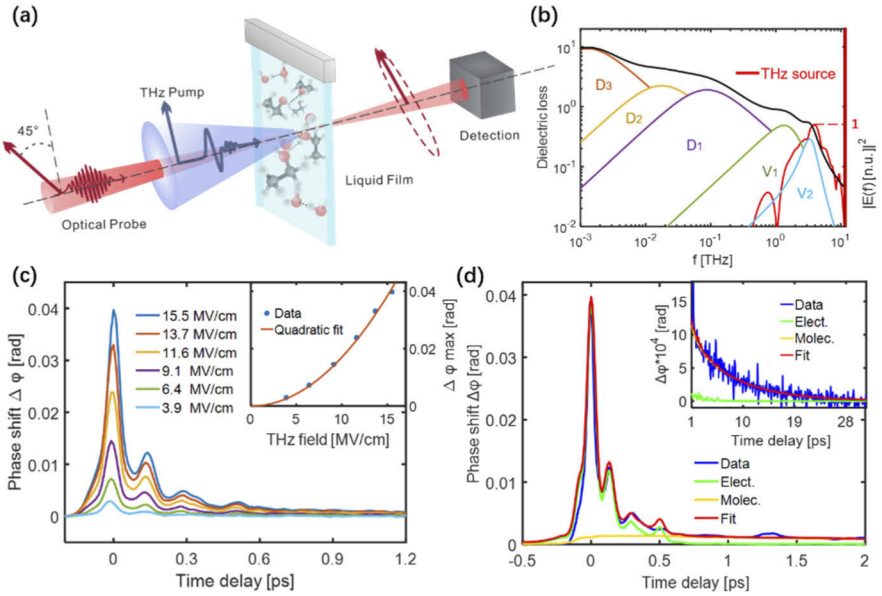

Fig. 1. (a) Diagram of the experimental system. About the liquid film: ethanol, water, and ethanol-water mixture. (b) The fitted dielectric loss spectrum of ethanol. The red line represents the frequency spectrum of the THz pump pulse in our experiment. (c) TKE responses of ethanol with different pump intensities. The inset shows the intensity-dependence curve of TKE response for ethanol. (d) The measured TKE response of ethanol (with the THz electric field strength of 15.5 MV/cm) and theoretical simulation results with electronic and molecular responses, respectively. The red line is the sum of the above two contributions, which matches well with the experimental data (blue line). The inset represents the TKE response of ethanol under a long observation time window, which is accompanied by a recovery process extending over tens of picoseconds.

The measured TKE signals of pure ethanol with different THz pump intensities are shown in Fig. 1(c). We record the peak values of the signals for different pump intensities and find that it is proportional to the square of the pump electric field strength (as shown in the inset of Fig. 1(c)), proving that the measured signals of pure ethanol are dominated by the THz Kerr

Optics EXPRESS

effect. In particular, the measured unipolar TKE signal of ethanol exhibits two characteristics: (i) a sharp rise at the sub-picosecond time scale, (ii) and a slow signal decay process that extends over tens of picoseconds. Usually, the characteristic (i) of sharp rise mainly comes from the electronic response of liquid itself, which is introduced by the electron cloud distortion under THz pump pulse excitation. Therefore, the temporal response of the electronic contribution at the sub-picosecond time scale should follow the THz intensity curve under ideal conditions. Furthermore, considering the inevitable error factors in the sampling process, such as the sampling error caused by the 50 fs probe pulse [32], the phase mismatch between THz pulse and 800 nm probe pulse [30,31], the surface reflection [31], and the Gouy phase shift during the propagation of the focused THz wave in the ethanol film [33,34], we correct the electronic response in ethanol as follows:

$$\Delta\varphi_e(t) = 2\pi B_e \int_0^l \left[t_{12}E(t+\beta x - \arctan(n_{THz}x/Z_{\mathrm{R}}))\cdot\exp(-\frac{\alpha}{2}x)\right]^2 dx \\ * \exp(-4\ln 2(t/\tau)^2) \tag{2}$$

where $B_e \approx 0.0093\times10^{-14}m/V^2$ represents the electronic response coefficient in ethanol [20], $t_{12} = 2/(n_{THz}+1)$ denotes the Fresnel transmission coefficient, and $n_{THz} \approx 1.47$ is the refractive index of THz wave in ethanol β≈0.53 ps/mm. is the phase mismatch factor between THz pulse and 800 nm probe pulse. $\exp(-\frac{\alpha}{2}x)$ signifies the attenuation of THz wave propagated in the sample (For ethanol, $\alpha \approx 140/cm$[35]). $\arctan(n_{THz}x/Z_R)$ denotes the phase shift term and Z_R is the Rayleigh length (~0.26 mm in this work). For broadband THz pulses, the phase factor of $\arctan(n_{THz}x/Z_R)$ is added to the time term of the THz electric field, which can be obtained by combining the derivative of the THz electric field with frequency-domain correction and trigonometric operations in the numerical calculation. $\exp(-4\ln 2(t/\tau)^2)$ represents the sampling pulse term and τ is the pulse width of the probe pulse (50 fs in this work). Here, we ignore the frequency dependence of these factors to reduce the huge amount of calculation, and use the optical parameters at the center frequency of 3.9 THz as the average value for approximation. Taking into account the above factors, we perform the convolution operation on the THz pulse term and the probe pulse term (Eq. (2)). The simulated electronic response is shown as the green line in Fig. 1(d) and is basically consistent with the measured TKE response under the sub-picosecond observation time window. Moreover, the frequency spectrum of applied broadband THz pulse covers a variety of molecular motion modes of ethanol. The dielectric loss spectrum of ethanol is shown in Fig. 1(b), which is fitted by three Debye-type contributions with relaxation times of ~100 ps, ~8 ps and ~1.1 ps, and two Lorentz contributions centered at~1.74 THz (V_1 mode) and~3.46 THz (V_2 mode). These contributions are attributed to the cooperative diffusion motion, fluctuations of terminal single monomers of the hydrogen bond chain structure, formation and breakage of hydrogen bonds, fluctuation of the alkyl group in the hydrogen bond chain-like network, and the intermolecular stretching vibration of the hydrogen bond network, respectively. The measured TKE signal (blue line) demonstrates no obvious gain from additional oscillation responses compared to the simulated electronic response at the sub-picosecond time scale, which indicates that the related vibrational modes (V_1, V_2 modes) are mainly isotropic [1,4,22].

In addition, the obvious decay characteristic (ii) of measured TKE signal in pure ethanol are dominated by the molecular motions of ethanol. The coupling between the permanent molecule dipole moment of ethanol and the THz electric field can be assigned to two fast Debye relaxation modes, which are related to the formation and breakage of hydrogen bonds with the relaxation time τ_1=1~2 ps, (D_1 process) and the fluctuations of terminal single monomers of the hydrogen bond chain structure with the relaxation time τ_2=7~12 ps (D_2 process) [1,25]. In the present work, we did not observe the slow Debye relaxation process associated with the reorganization of the hydrogen bond network with a time constant up to ~100 ps (D_3 process), which is not

Optics EXPRESS

effectively identified by the used THz pump pulses. We use a double exponential decay model [36] to describe the molecular contributions of the two fast Debye relaxation modes to the TKE signal of ethanol, and the fitted time constants of τ_1=1.1 ps, τ_2=8 ps are adopted [25]. The simulated molecular response of ethanol is demonstrated as the yellow line in Fig. 1(d). Moreover, we find that the sum (red curve) of simulated electronic and molecular responses is in good agreement with the measured TKE signal (blue). This indicates that the electronic contribution is absolutely dominant in the ultrafast evolution process at the sub-picosecond time scale, and the molecular contribution plays the major role over tens of picoseconds. Note that Kampfrath et al. also observed that the unipolar TKE signal of ethanol is dominated by the electronic response under a THz pump field with ~1 THz center frequency [22]. However, Zalden et al. used THz pulses with ~0.25 THz center frequency to excite ethanol and obtained a bipolar TKE signal with relatively high molecular response component [20], revealing that the molecular response of ethanol TKE signal depends heavily on the driving frequency.

Based on the above TKE measurement results of ethanol, we investigate the TKE responses of the ethanol-water mixtures with different molar proportions under THz pulse excitation (with the electric field strength of 15.5 MV/cm), as shown in Fig. 2(a). The mixed ratio of the two liquids is expressed by the molar concentration C of ethanol molecules, namely C=100 mol % (ethanol), C=0 mol % (water). To facilitate the observation of the decay characteristics, we normalize the measured TKE response of the ethanol-water mixtures with the molar concentration of 100, 70, 40 mol % according to the amplitude at t=5 ps, respectively (as shown in the inset of Fig. 2(a)). The TKE responses for the ethanol-water mixtures with different molar concentrations almost overlap after ~5 ps, indicating that the molecular responses of the mixtures are still dominated by the two fast Debye relaxation modes of ethanol. Firstly, we use Eq. (3) to fit the TKE responses of ethanol-water mixtures with different molar concentrations and the corresponding fitted results are shown by the gray lines in Fig. 2(b).

$$\Delta\varphi(t) = a_i\Delta\varphi_{water}(t) + b_i\Delta\varphi_{ethanol}(t) \tag{3}$$

where $\Delta\varphi_{water}(t)$ represents the measured TKE response of pure water (C=0 mol %, as shown by the wathet blue line in Fig. 2). The experimental and theoretical research of the TKE response in water has been reported in our latest study, in which the measured bipolar signal is assigned to the electric, Debye relaxation, intermolecular hydrogen bond stretching vibration and bending vibration contributions [23]. In particular, the transient birefringence is mainly attributed to the two modes of intermolecular hydrogen bond motions [23]. $\Delta\varphi_{ethanol}(t)$ denotes the measured TKE response of ethanol (C=100 mol %), which can reach about ~10 times greater than that of water under the same condition. a_i and b_i represent the coefficients related to the ethanol molar concentration in the mixture. Under the ultrafast time window, the contributions of water and ethanol to the TKE response depend on the number of two types of excited molecules, which are mainly related to the molar concentration of ethanol and the THz absorption coefficient of the ethanol-water mixture. Therefore, the fitted TKE responses of the ethanol-water mixtures with different molar concentration are present in Fig. 2(b), (c). On the sub-picosecond time scale (before 1 ps), the fitted results are in good agreement with the measured data for different molar concentrations (Fig. 2(b)), indicating that the temporal evolution curves of the TKE responses of the mixtures can always be represented by the linear superposition of the TKE responses of pure water and ethanol.

However, if this linear superposition simulation is extended to the time scale over tens of picoseconds (after 1 ps), the measured results with different molar concentrations deviate from the expectations. For example, as shown in Fig. 2(c), the measured TKE response of the ethanol-water mixture at C=70 mol % (red line) is greater than the calculated value (gray line), while the measured TKE response at C=40 mol % (yellow line) is smaller than the calculated value (gray line). The similar deviation from the linear superposition simulation has also been

Optics EXPRESS

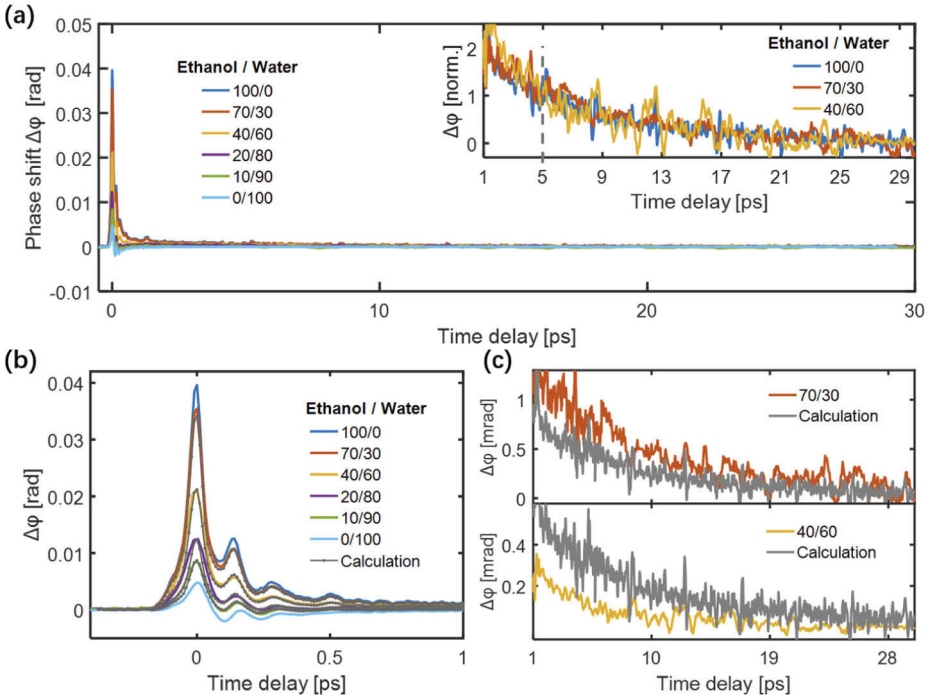

Fig. 2. (a) TKE responses of ethanol-water mixtures with different molar ratio of ethanol/water molecules. The inset shows the normalized TKE responses of the ethanol-water mixtures (normalization according to the amplitude at t=5 ps, respectively) with the molar ratios of 100/0, 70/30 and 40/60 (corresponding to the ethanol molar concentrations of 100, 70 and 40 mol% respectively). (b) The fitted (gray lines) and measured TKE responses of ethanol-water mixtures with different molar ratios under the sub-picosecond observation time window (before 1 ps). (c) The measured TKE responses of ethanol-water mixtures (with the molar ratios of 70/30 and 40/60) and the corresponding calculated results (gray lines) under the observation time window over tens of picoseconds (after 1 ps).

observed in the Raman spectrum study of ethanol-water mixtures below 40 cm^{-1} [37], implying that there are complex interactions related to the molecular structures in the mixture.

To further fully investigate the potential molecular motions, we then discuss the TKE responses under the observation time windows of sub-picosecond and tens of picoseconds separately. t=1 ps is the break point of the two observation time windows. On the sub-picosecond time scale (before 1 ps), the fitted values of a_i, b_i are depicted in Fig. 3(a). With the amount of water molecules increases, the contribution of water to the TKE response of the mixture gradually increases, indicating that the restricted translational motion of adjacent water molecules contributes incrementally to the anisotropic response with the THz pulse excitation. A small amount of ethanol molecules in the mixture will hardly affect the hydrogen bond network of liquid water. Even with the addition of a large amount of ethanol molecules, the TKE response of the mixture still contains the anisotropy information about the water-water intermolecular hydrogen bond motion modes, implying that the water intermolecular hydrogen bond structure can exist in the ethanol-rich region. These measurements under sub-picosecond observation time window are basically consistent with the results of the low-frequency Raman studies for the ethanol-water mixture, which show that the intermolecular vibrational modes are independent of each other in the mixture of these two liquids [37,38].

Optics EXPRESS

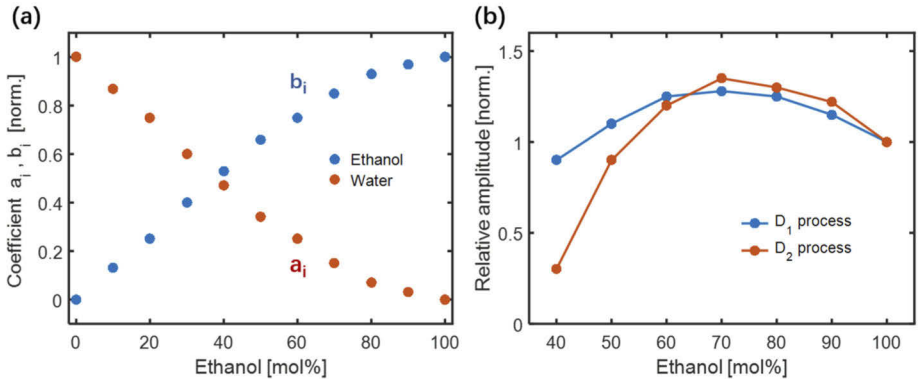

Fig. 3. (a) Coefficients a_i, b_i for different molar concentrations under the sub-picosecond observation time window. (b) The relative amplitudes of two Debye relaxation processes at different molar concentrations compared to pure ethanol.

Under the observation time window over tens of picoseconds, we use a double exponential decay model (Eq. (4)) to simulate the relaxation processes in the ethanol-water mixtures with different molar concentrations. This fitting method has been proved appropriate in the recent molecular dynamics simulation research [25].

$$\Delta\varphi_{\mathrm{m}}(t) \propto E^2(t) * M(A_{c=i}/\tau_1 \exp(-t/\tau_1) + B_{c=i}/\tau_2 \exp(-t/\tau_2)) \tag{4}$$

On the premise that the fitted curve and the measured data are in good agreement (such as the fitting results of pure ethanol under the window over tens of picoseconds shown in the inset of Fig. 1(d)), we obtain the same values of time constants (τ_1=1.1 ps, τ_2=8 ps) for the mixtures with different molar concentrations and record the amplitudes of $A_{C=i}$, $B_{C=i}$ related to the two molecular relaxation modes ($C = i$ represents the ethanol molar concentration of the ethanol-water mixture). Here we ignore the contribution of the Debye relaxation process of water to the anisotropic response, because the response on the picosecond scale of water is too small compared to ethanol (for example, the response of water at t=5 ps is less than one-twentieth that of pure ethanol). In order to more directly quantify and analyze the deviations in mixtures of different molar concentrations (as shown in Fig. 2(c)), the recorded amplitudes of $A_{C=i}$, $B_{C=i}$ are divided by a concentration-related linear fitting value to obtain the values of $A_{C=i}'$, $B_{C=i}'$ (i.e., $A_{C=i}' = A_{C=i}/(A_{C=1}b_i)$, $B_{C=i}' = B_{C=i}/(B_{C=1}b_i)$, and the parameter b_i is taken from Fig. 3(a)), which represent the relative amplitudes of two Debye relaxation processes at different molar concentrations ($C = i$) compared to pure ethanol. Here we take b_i as the normalization coefficient of $A_{C=i}'$, $B_{C=i}'$ to illustrate the changes of the amplitudes of the two Debye relaxation processes when the excited ethanol molecules in ethanol-water mixtures with different molar concentrations are the same. As shown in Fig. 3(b), the blue line represents the relative amplitude $A_{C=i}'$ for D_1 relaxation process with different molar concentrations. When adding a small amount of water molecules to ethanol, we observe a relatively enhanced D_1 relaxation process, which is due to the increased molecular motions associated with the hydrogen bond breakage and formation of ethanol. However, as the amount of water molecules increases, the relative amplitude of D_1 relaxation process decreases, and an inflection point appears at around ~70 mol%. For the relative amplitude $B_{C=i}'$ of D_2 relaxation process depicted by the red line in Fig. 3(b), it is associated with the fluctuations of terminal ethanol monomers of the hydrogen bond chain. When a small amount of water molecules is introduced into ethanol, the relative amplitude increases as the molar concentration of ethanol decreases in the range of C=100~70 mol %. However, with the

Optics EXPRESS

number of water molecules increases, the relative amplitude gradually decreases in the range of C=70~30 mol % and quickly drop to the noise level when C is less than ~30 mol %.

The relative amplitudes of D_1 and D_2 relaxation processes are closely related to the hydrogen bond chain structure of ethanol in the mixed solution. In pure ethanol, the ratio between the number of ethanol intermolecular hydrogen bonds and the number of ethanol molecules is about 95% [25,39]. Meanwhile, the number of terminal ethanol monomers of the hydrogen bond chain accounts for about 10% of the number of ethanol molecules [25,39]. The addition of a small amount of water molecules (in the range of C=100~70 mol %) causes the long hydrogen bond chain of ethanol to break into several short chains, thereby increasing the number of terminal ethanol monomers of chains and the probability of formation and breakage of ethanol intermolecular hydrogen bonds. Therefore, the relative amplitudes of D_1 and D_2 relaxation processes increase almost simultaneously. According to our experimental results, at the inflection point of 70 mol %, the proportion of terminal ethanol monomers of the hydrogen bond chain increases to about 14% compared with that in pure ethanol, which is basically consistent with the growth trend of molecular dynamics simulation [25,39]. When water molecules are further added (in the range of C=70~30 mol %), the amount of free ethanol monomers isolated by water molecules gradually increases, resulting in the decrease in the proportion of terminal ethanol monomers of the chain. When the molar concentration of ethanol reduces below 30 mol%, the amplitude of D_2 relaxation process has been decreased to the noise level. This is mainly because ethanol molecular clusters are gradually dissolved by water molecules, making it difficult to maintain the chain-like structure of ethanol. As a result, this relaxation mechanism of D_2 process vanishes as water molecules dominate the mixture. Nonetheless, a large number of free ethanol monomers still have the opportunity to combine with other ethanol molecules to form hydrogen bonds. Therefore, compared with the rapid decrease of the amplitude of D_2 process, the decreasing rate of the amplitude for D_1 process is relatively slow. In addition, the characteristic time constant is not significantly affected by the length of the hydrogen bond chain. The nearly stable time constant in the ethanol-water mixtures with different molar concentrations of ethanol is also supported by the recent study [25].

3. Conclusion

The intense broadband THz pulses induce the Kerr effect in ethanol and ethanol-water mixtures, which provides a time-resolved perspective for exploring the dynamics of collective or cooperative movement of molecules in hydrogen bond liquids. The TKE measurement of ethanol on the sub-picosecond time scale shows that the vibrational modes related to the stretching vibration of the hydrogen bond network and the fluctuation of the alkyl group in the hydrogen bond chain-like network, have no harmonic oscillator characteristics and no obvious gain in response amplitude, indicating that these vibrational modes are mainly isotropic. For the ethanol-water mixtures with different molar proportions, the anisotropic contribution related to the intermolecular hydrogen bond movement of water can always be observed, which demonstrates that water intermolecular hydrogen bond structure can exist even in the ethanol-rich region. Moreover, the relative molecular contributions of ethanol related to the relaxation processes show a trend of first increasing and then decreasing with the addition of water molecules, which reflects the breakage of the hydrogen bonds and the destruction of chain-like structure of ethanol. This work presents a new perspective for exploring the interaction of solute-solvent molecules, and provides experimental references for the establishment of expanded theoretical models associated with the molecular dynamics of hydrogen bond liquids.

Funding. National Natural Science Foundation of China (12074272, 61935001, 61905271); Beijing Municipal Natural Science Foundation (JQ18015); Guangdong Basic and Applied Basic Research Foundation (2020A1515011083); National Key Research and Development Program of China (2020YFB2009303).

Disclosures. The authors declare no conflicts of interest.

Optics EXPRESS

Data availability. The data underlying the results presented herein are not publicly available currently but can be obtained from the authors upon reasonable request.

References

1. T. Fukasawa, T. Sato, J. Watanabe, Y. Hama, W. Kunz, and R. Buchner, "Relation between dielectric and low-frequency Raman spectra of hydrogen-bond liquids," Phys. Rev. Lett. **95**(19), 197802 (2005).
2. H. Elgabarty, T. Kampfrath, D. J. Bonthuis, V. Balos, N. K. Kaliannan, P. Loche, R. R. Netz, M. Wolf, T. D. Kühne, and M. Sajadi, "Energy transfer within the hydrogen bonding network of water following resonant terahertz excitation science advance," Sci. Adv. **6**(17), eaay7074 (2020).
3. F. Novelli, L. R. Pestana, K. C. Bennett, F. Sebastiani, E. M. Adams, N. Stavrias, T. Ockelmann, A. Colchero, C. Hoberg, G. Schwaab, T. H. Gordon, and M. Havenith, "Strong anisotropy in liquid water upon librational excitation using terahertz laser fields," J. Phys. Chem. B **124**(24), 4989–5001 (2020).
4. Y. Yomogida, Y. Sato, R. Nozaki, T. Mishina, and J. Nakahara, "Dielectric study of normal alcohols with THz time-domain spectroscopy," J. Mol. Liq. **154**(1), 31–35 (2010).
5. F. Perakis, L. D. Marco, A. Shalit, F. Tang, Z. R. Kann, T. D. Kühne, R. Torre, M. Bonn, and Y. Nagata, "Vibrational spectroscopy and dynamics of water," Chem. Rev. **116**(13), 7590–7607 (2016).
6. M. C. Bellissent-Funel, A. Hassanali, M. Havenith, R. Henchman, P. Pohl, F. Sterpone, D. van der Spoel, Y. Xu, and A. E. Garcia, "Water determines the structure and dynamics of proteins," Chem. Rev. **116**(13), 7673–7697 (2016).
7. K. Stokely, M. G. Mazza, H. E. Stanley, and G. Franzese, "Effect of hydrogen bond cooperativity on the behavior of water," Proc. Natl. Acad. Sci. U. S. A. **107**(4), 1301–1306 (2010).
8. S. Takaaki and R. Buchner, "Dielectric relaxation processes in ethanol/water mixtures," J. Phys. Chem. A **108**(23), 5007–5015 (2004).
9. V. Balos, G. Bierhance, M. Wolf, and M. Sajadi, "Terahertz-magnetic-field induced ultrafast faraday rotation of molecular liquids," Phys. Rev. Lett. **124**(9), 093201 (2020).
10. K. Lin, N. Hu, X. Zhou, S. Liu, and Y. Luo, "Reorientation dynamics in liquid alcohols from Raman spectroscopy," J. Raman Spectrosc. **43**(1), 82–88 (2012).
11. M. Nedic, T. N. Wassermann, R. W. Larsen, and M. A. Suhm, "Combined Raman-and infrared jet study of mixed methanol-water and ethanol-water clusters," Phys. Chem. Chem. Phys. **13**(31), 14050–14063 (2011).
12. Y. L. Rezus and H. J. Bakker, "Observation of immobilized water molecules around hydrophobic groups," Phys. Rev. Lett. **99**(14), 148301 (2007).
13. H. Shirota, K. Yoshihara, N. A. Smith, S. Lin, and S. R. Meech, "Deuterium isotope effects on ultrafast polarisability anisotropy relaxation in methanol," Chem. Phys. Lett. **281**(1-3), 27–34 (1997).
14. C. J. Fecko, J. D. Eaves, and A. Tokmakoff, "Isotropic and anisotropic Raman scattering from molecular liquids measured by spatially masked optical Kerr effect spectroscopy," J. Chem. Phys. **117**(3), 1139–1154 (2002).
15. K. N. Woods and H. Wiedemann, "The influence of chain dynamics on the far-infrared spectrum of liquid methanol-water mixtures," J. Chem. Phys. **123**(13), 134507 (2005).
16. T. Sato, A. Chiba, and R. Nozaki, "Dynamical aspects of mixing schemes in ethanol-water mixtures in terms of the excess partial molar activation free energy, enthalpy, and entropy of the dielectric relaxation process," J. Chem. Phys. **110**(5), 2508–2521 (1999).
17. J. A. Larkin, "Thermodynamic properties of aqueous non-electrolyte mixtures in. excess enthalpy for water + ethanol at 298.15 to 383.15 K," J. Chem. Thermodyn. **7**(2), 137–148 (1975).
18. Y. Marcus, "Water structure enhancement in water-rich binary solvent mixtures. Part II. the excess partial molar heat capacity of the water," J. Mol. Liq. **166**, 62–66 (2012).
19. G. Guevara-Carrion, J. Vrabec, and H. Hasse, "Prediction of self diffusion coefficient and shear viscosity of water and its binary mixtures with methanol and ethanol by molecular simulation," J. Chem. Phys. **134**(7), 074508 (2011).
20. P. Zalden, L. Song, X. Wu, H. Huang, F. Ahr, O. D. Mücke, J. Reichert, M. Thorwart, P. K. Mishra, R. Welsch, R. Santra, F. X. Kärtner, and C. Bressler, "Molecular polarizability anisotropy of liquid water revealed by terahertz-induced transient orientation," Nat. Commun. **9**(1), 2142 (2018).
21. M. Sajadi, M. Wolf, and T. Kampfrath, "Transient birefringence of liquids induced by terahertz electric-field torque on permanent molecular dipoles," Nat. Commun. **8**(1), 14963 (2017).
22. T. Kampfrath, R. K. Campen, M. Wolf, and M. Sajadi, "The nature of the dielectric response of methanol revealed by the terahertz Kerr effect," J. Phys. Chem. Lett. **9**(6), 1279–1283 (2018).
23. H. Zhao, Y. Tan, L. Zhang, R. Zhang, M. Shalaby, C. Zhang, Y. Zhao, and X.-C. Zhang, "Ultrafast hydrogen bond dynamics of liquid water revealed by terahertz-induced transient birefringence," Light: Sci. Appl. **9**(1), 136 (2020).
24. H. Zhao, Y. Tan, R. Zhang, Y. Zhao, C. Zhang, and L. Zhang, "Anion-water hydrogen bond vibration revealed by the terahertz Kerr effect," Opt. Lett. **46**(2), 230–233 (2021).
25. J. Cardona, M. B. Sweatman, and L. Lue, "Molecular dynamics investigation of the influence of the hydrogen bond networks in ethanol/water mixtures on dielectric spectra," J. Phys. Chem. B **122**(4), 1505–1515 (2018).
26. A. Y. Zasetsky, A. S. Lileev, and A. K. Lyashchenko, "Molecular dynamic simulations of terahertz spectra for water-methanol mixtures," Mol. Phys. **108**(5), 649–656 (2010).
27. R. Li, C. D' Agostino, J. McGregor, M. D. Mantle, J. A. Zeitler, and L. F. Gladden, "Mesoscopic structuring and dynamics of alcohol/water solutions probed by terahertz time-domain spectroscopy and pulsed field gradient nuclear magnetic resonance," J. Phys. Chem. B **118**(34), 10156–10166 (2014).

Optics EXPRESS

28. M. Shalaby and C. P. Hauri, "Demonstration of a low-frequency three-dimensional terahertz bullet with extreme brightness," Nat. Commun. **6**(1), 5976 (2015).
29. Q. Jin, Y. E Williams, K. , J. Dai, and X. C. Zhang, "Observation of broadband terahertz wave generation from liquid water," Appl. Phys. Lett. **111**(7), 071103 (2017).
30. H. J. Bakker, G. C. Cho, H. Kurz, Q. Wu, and X. C. Zhang, "Distortion of THz pulses in electro-optic sampling," J. Opt. Soc. Am. B **15**(6), 1795–1801 (1998).
31. M. Sajadi, M. Wolf, and T. Kampfrath, "Terahertz-field-induced optical birefringence in common window and substrate materials," Opt. Express **23**(22), 28985–28992 (2015).
32. R. Buchner and J. Barthel, "Kinetic processes in the liquid phase studied by high frequency permittivity measurements," J. Mol. Liq. **63**(1-2), 55–75 (1995).
33. Y. Tan, H. Zhao, R. Zhang, C. Zhang, Y. Zhao, and L. Zhang, "Ultrafast optical pulse polarization modulation based on the terahertz-induced Kerr effect in low-density polyethylene," Opt. Express **28**(23), 35330–35338 (2020).
34. S. Ahmed, J. Savolainen, and P. Hamm, "The effect of the Gouy phase in optical-pump-THz-probe spectroscopy," Opt. Express **22**(4), 4256–4266 (2014).
35. E. Sani and A. Dell'Oro, "Spectral optical constants of ethanol and isopropanol from ultraviolet to far infrared," Opt. Mater. **60**, 137–141 (2016).
36. A. Migus, Y. Gauduel, and J. L. Martin, "Excess electrons in liquid water: first evidence of a prehydrated state with femtosecond lifetime," Phys. Rev. Lett. **58**(15), 1559–1562 (1987).
37. Y. Amo and Y. Tominaga, "Low-frequency Raman study of ethanol-water mixture," Chem. Phys. Lett. **320**(5-6), 703–706 (2000).
38. K. Egashira and N. Nishi, "Low-frequency raman spectroscopy of ethanol-water binary solution: evidence for self-association of solute and solvent molecules," J. Phys. Chem. B **102**(21), 4054–4057 (1998).
39. O. Gereben and L. Pusztai, "Cluster formation and percolation in ethanol-water mixtures," Chem. Phys. **496**(17), 1–8 (2017).